symmetry

MDPI

Article

# Chiral Oscillations and Spontaneous Mirror Symmetry Breaking in a Simple Polymerization Model

**William Bock and Enrique Peacock-López** *

Department of Chemistry, Williams College, Williamstown, MA 01267, USA; wb3@williams.edu
* Correspondence: epeacock@williams.edu

Received: 10 July 2020; Accepted: 19 August 2020; Published: 20 August 2020

**Abstract:** The origin of biological homochirality—defined as the preference of biological systems for only one enantiomer—has widespread implications in the study of chemical evolution and the origin of life. The activation—polymerization—epimerization—depolymerization (APED) model is a theoretical model originally proposed to describe chiral symmetry breaking in a simple dimerization system. It is known that the model produces chiral and chemical oscillations for certain system parameters, in particular, the preferential formation of heterochiral polymers. In order to investigate the effect of higher oligomers, our model adds trimers, tetramers, and pentamers. We report sustained oscillations of all chemical species and the enantiomeric excess for a wide range of parameter sets as well as the periodic chiral amplification of a small initial enantiomeric excess to a nearly homochiral state.

**Keywords:** chiral oscillations; spontaneous mirror symmetry breaking; origin of homochirality

## 1. Introduction

The origin of biological homochirality has attracted researchers' attentions for decades. At the center of this issue lies the question of how an optically inactive mixture—that is, a mixture containing equal amounts of two enantiomers—can react in such a way that propagates a small initial enantiomeric excess (*ee*) to form a product that is enantiopure. The quest for a mechanism that could have caused such spontaneous mirror symmetry breaking (SMSB) in a prebiotic environment has spurred decades of theoretical and experimental research. In Frank's seminal paper [1], he introduced a simple model capable of SMSB, in which enantiomers L and D catalyze their own formation, and they inhibit each other by forming the non-reactive heterochiral dimer LD. The latter step, which Frank termed "mutual antagonism", is crucial for chiral amplification, because the formation of the heterodimer is a greater penalty for the rarer enantiomer, allowing the common one to predominate.

Frank's paradigmatic scheme has inspired many variations and extensions, including several theoretical models investigating symmetry breaking in the famous Soai reaction [2]. In one such model, homochiral dimers are formed in addition to heterochiral ones and dimerization is reversible [3]. Models have also been proposed in which the monomers themselves are not autocatalytic, but instead homochiral dimers catalyze the formation of monomers of the same chirality [4,5].

The same paradigm has also been extended to systems involving longer polymers made up of amino acids or nucleotides. In one influential polymerization model, only the longest homochiral polymers catalyze the formation of chiral monomers, and mutual antagonism takes the form of enantiomeric cross inhibition, whereby the addition of a wrong-handed monomer to a growing chain halts elongation of that chain [6]. Many variations of this model have since been proposed [7,8], including one in which homochirality arises in concert with the emergence of life [9].

In this article, we study a toy polymerization model introduced by Plasson et al. that stands out from the aforementioned ones, in that it does not involve direct catalysis in monomer synthesis [10]. Instead, it introduces autocatalytic behavior through the presence of stereoselective epimerization reactions, whereby heterodimers LD and DL epimerize at the N-terminal residue to form homodimers DD and LL, respectively. In this case, the position adjacent to the epimerizing center can be considered an autocatalyst, because it converts the opposite enantiomer to its own chirality. These epimerization reactions, along with polymerization and hydrolysis, introduce both the autocatalytic behavior and mutual inhibition necessary for the destabilization of the racemic state [10,11].

The system is composed of activation, polymerization, epimerization, and depolymerization (APED) reactions between deactivated monomers L and D; activated monomers L* and D*; and dimers LL, DD, DL, and LD, where L and D represent enantiomers and DL and LD have the same chemical properties:

$$L \xrightarrow{a} L^* \qquad LL \xrightarrow{h} L + L \tag{1}$$

$$D \xrightarrow{a} D^* \qquad DD \xrightarrow{h} D + D \tag{2}$$

$$L^* \xrightarrow{b} L \qquad LD \xrightarrow{\beta h} L + D \tag{3}$$

$$D^* \xrightarrow{b} D \qquad DL \xrightarrow{\beta h} D + L \tag{4}$$

$$L + L^* \xrightarrow{p} LL \qquad LL \xrightarrow{\gamma e} DL \tag{5}$$

$$D + D^* \xrightarrow{p} DD \qquad DD \xrightarrow{\gamma e} LD \tag{6}$$

$$L + D^* \xrightarrow{\alpha p} DL \qquad DL \xrightarrow{e} LL \tag{7}$$

$$D + L^* \xrightarrow{\alpha p} LD \qquad LD \xrightarrow{e} DD \tag{8}$$

The model is contained within a closed system with a fixed concentration, and the rates of polymerization, depolymerization and epimerization are different for their homo- and heterochiral counterparts (i.e., they are stereoselective).

Although Plasson et al.'s report searches for the monotonic emergence of chiral states, they note that oscillations of all chemical species, and the enantiomeric excess, occur when heterochiral dimers are strongly preferred. These oscillations are the focus of Stich et al.'s report, which performs a comprehensive bifurcation analysis and finds that oscillations occur for a wide range of parameter sets [12]. Such chiral oscillatory phenomena have important implications for the transmission of chirality in chemical systems: in contrast to models for SMSB that involve the monotonic emergence of chiral steady states, systems involving chiral oscillations add another layer of stochasticity to the final sign of chirality that is ultimately transmitted to the system. This is because the memory of the sign of any initial fluctuation is erased by subsequent oscillations. In recent years, chiral oscillations have been of growing interest in theoretical models [12,13], especially in light of experimental evidence of chiral oscillations in the polymerization of some amino acids [14].

The APED model is a powerful tool for studying chiral oscillatory phenomena because its simplicity makes it amenable to the comprehensive mathematical analysis of its parameters, which can provide insight into the driving forces behind real chemical systems involving chiral oscillations. Despite laying the groundwork for describing chiral oscillations in polymerization systems, its restriction to dimers makes it unable to encapsulate the nuances that result from the formation of higher oligomers. One experimental study [15], for example, shows that the stereoselectivities of epimerization and hydrolysis for some amino acids differ between di- and tripeptides. Introducing trimers to the model takes one step closer to capturing such nuances while preserving the simplicity and applicability of the original APED scheme.

This article is organized as follows. In Section 2, we introduce the expanded APED model and demonstrate chiral and chemical oscillations in the expanded model. In Section 3, we analyze the bifurcation diagrams of several system parameters and then expand the model further to examine the onset of oscillations in the presence of tetramers and pentamers. In Section 4, we explore the minimum initial enantiomeric excess required to produce oscillations in the minimal and expanded APED models. We also demonstrate large amplitude oscillations in the overall enantiomeric excess, which can periodically achieve near homochirality ($ee > 0.98$). Finally, we close the article with a discussion of the results in Section 5.

## 2. The Expanded APED Model

The APED model was originally introduced to describe the monotonic chiral symmetry breaking of peptides, in contrast to the chiral oscillations presented in this report (and originally presented by Stich et al.). This discrepancy results from Plasson et al.'s assumption that amino acids tend to condense into homochiral peptides faster than heterochiral ones. Although this can be true [16,17], experimental evidence involving the condensation of phenylglycine reports damped chiral and chemical oscillations by peptides, and it has been suggested that the oscillations are caused by an APED-like system that favors the formation of heterochiral peptides [14].

To our knowledge, the numerous applications and variations of the APED model have all been limited to dimers [10,12,14]. Although the APED is strictly a toy model [18], the inclusion of higher oligomers can more accurately simulate real polymerization systems while preserving the simplicity and generality of the APED scheme, which is what lends itself well to the systematic analysis of the parameters (presented in Section 3).

We assume that polymerization in the expanded model is restricted by enantiomeric cross-inhibition; that is, only homochiral chains are capable of polymerization, and the addition of a monomer of the opposite chirality halts elongation of that chain. This phenomenon has been shown in the oligomerization of activated mononucleotides [19]. Furthermore, in order to maintain the model's simplicity, polymerization is unidirectional and is limited to monomer addition. The reactions we add to the system are represented by the following equations.

$$LL + L^* \xrightarrow{p_2} LLL \qquad DLL \xrightarrow{\beta_2 h_2} D + LL \tag{9}$$

$$DD + D^* \xrightarrow{p_2} DDD \qquad LDD \xrightarrow{\beta_2 h_2} L + DD \tag{10}$$

$$LL + D^* \xrightarrow{\alpha_2 p_2} DLL \qquad DLL \xrightarrow{e_2} LLL \tag{11}$$

$$DD + L^* \xrightarrow{\alpha_2 p_2} LDD \qquad LDD \xrightarrow{e_2} DDD \tag{12}$$

$$LLL \xrightarrow{h_2} L + LL \qquad LLL \xrightarrow{\gamma_2 e_2} DLL \tag{13}$$

$$DDD \xrightarrow{h_2} D + DD \qquad DDD \xrightarrow{\gamma_2 e_2} LDD \tag{14}$$

Our expansion introduces homo- and heterochiral trimers, and the new reactions include homochiral polymerization (rate $p_2$), heterochiral polymerization (rate $\alpha_2 p_2$), homochiral hydrolysis (rate $h_2$), heterochiral hydrolysis (rate $\beta_2 h_2$), homochiral epimerization (rate $e_2$), and heterochiral epimerization (rate $\gamma_2 e_2$). Similar to the original APED model, mass is conserved so that the total concentration $c$ = [L] + [D] + [L*] + [D*] + 2([LL] + [DD] + [LD] + [DL]) + 3([LLL] + [DDD] + [LDD] + [DLL]) is constant. The enantiomeric excess is defined as $ee$ = [L] + [L*] + 2[LL] + 3[LLL] + [DLL] - ([D] + [D*] + 2[DD] + 3[DDD] + [LDD])/c.

The trimer reactions in conjunction with the original APED model transcribe into the following set of ordinary differential equations,

$$\begin{aligned}\frac{d[L]}{dt} &= -a[L] - p_1[L][L^*] - \alpha_1 p_1[L][D^*] + 2h_1[LL] + b[L^*] + \beta_1 h_1[DL] \\ &\quad +\beta_1 h_1[LD] + \beta_2 h_2[LDD] + h_2[LLL] \end{aligned} \tag{15}$$

$$\begin{aligned}\frac{d[D]}{dt} &= -a[D] - p_1[D][D^*] - \alpha_1 p_1[D][L^*] + 2h_1[DD] + b[D^*] \\ &\quad +\beta_1 h_1[DL] + \beta_1 h_1[LD] + \beta_2 h_2[DLL] + h_2[DDD] \end{aligned} \tag{16}$$

$$\begin{aligned}\frac{d[L^*]}{dt} &= a[L] - b[L^*] - \alpha_1 p_1[L^*][D] - p_2[LL][L^*] \\ &\quad -p_1[L][L^*] - \alpha_2 p_2[DD][L^*] \end{aligned} \tag{17}$$

$$\begin{aligned}\frac{d[D^*]}{dt} &= a[D] - b[D^*] - \alpha_1 p_1[D^*][L] - p_2[DD][D^*] \\ &\quad -p_1[D][D^*] - \alpha_2 p_2[LL][D^*] \end{aligned} \tag{18}$$

for the dimers,

$$\begin{aligned}\frac{d[LL]}{dt} &= p_1[L][L^*] - h_1[LL] + e_1[DL] - p_2[LL][L^*] \\ &\quad -\gamma_1 e_1[LL] + h_2[LLL] - \alpha_2 p_2[LL][D^*] + \beta_2 h_2[DLL] \end{aligned} \tag{19}$$

$$\begin{aligned}\frac{[DD]}{dt} &= p_1[D][D^*] - h_1[DD] + e_1[LD] - p_2[DD][D^*] \\ &\quad -\gamma_1 e_1[DD] + h_2[DDD] - \alpha_2 p_2[DD][L^*] + \beta_2 h_2[LDD] \end{aligned} \tag{20}$$

$$\frac{[DL]}{dt} = \alpha_1 p_1[L][D^*] - e_1[DL] - \beta_1 h_1[DL] + \gamma_1 e_1[LL] \tag{21}$$

$$\frac{[LD]}{dt} = \alpha_1 p_1[D][L^*] - e_1[LD] - \beta_1 h_1[LD] + \gamma_1 e_1[DD] \tag{22}$$

and finally for the trimers,

$$\frac{[LLL]}{dt} = p_2[LL][L^*] - h_2[LLL] + e_2[LLD] - \gamma_2 e_2[LLL] \tag{23}$$

$$\frac{[DDD]}{dt} = p_2[DD][D^*] - h_2[DDD] + e_2[DDL] - \gamma_2 e_2[DDD] \tag{24}$$

$$\frac{[DLL]}{dt} = \alpha_2 p_2[LL][D^*] - \beta_2 h_2[DLL] - e_2[DLL] + \gamma_2 e_2[LLL] \tag{25}$$

$$\frac{[LDD]}{dt} = \alpha_2 p_2[DD][L^*] - \beta_2 h_2[LDD] - e_2[LDD] + \gamma_2 e_2[DDD] \tag{26}$$

Oscillations for the expanded APED model are illustrated in Figure 1, which displays the concentration of the homochiral trimers DDD and LLL as well as the overall enantiomeric excess. For parameter values, we choose $\alpha_1 = \alpha_2 = 50$, $a = p_1 = h_1 = e_1 = p_2 = h_2 = e_2 = 1$, $b = \beta_1 = \gamma_1 = \beta_2 = \gamma_2 = 0$, $c$ = 0.5, and we keep a = 1 and b = 0 for the remainder of the article. In this case, we use an initial enantiomeric excess of $ee_{init}$ = 0.01, and we see that this initial excess is propagated to oscillations ranging from $ee \approx -0.6$ to 0.6 within 200 dimensionless time increments. In Section 4, we show that the amplitude of oscillations in *ee* increases substantially as higher oligomers are introduced to the system.

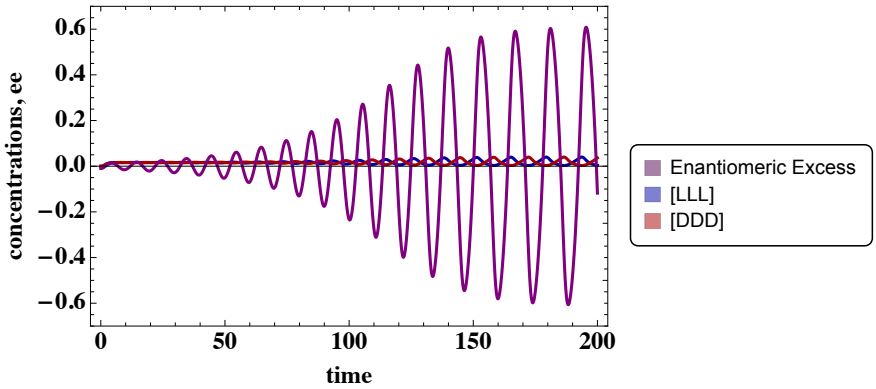


**Figure 1.** Stable oscillations of the concentrations of LLL and DDD as well as the enantiomeric excess (*ee*) for the parameter values $\alpha_1 = \alpha_2 = 20, a = h_1 = e_1 = p_1 = p_2 = h_2 = e_2 = 1, b = \beta_1 = \gamma_1 = \beta_2 = \gamma_2 = 0$, $c$ = 0.5 and $ee_{init} = 0.01$. For simplicity we only display [LLL] and [DDD], although all concentrations oscillate. The units for time are dimensionless, because we do not use literature values for the reaction rates.

## 3. Bifurcation Analysis

### *3.1. Trimer Model*

Using Stich et al.'s bifurcation analysis of the minimal APED model as a platform, in this section we present our bifurcation analysis of several system parameters to determine how general is the appearance of oscillations in the expanded model. In particular, we focus on the relative stereoselectivities of polymerization, epimerization, and hydrolysis, namely, $\alpha_1$ and $\alpha_2$, $\gamma_1$ and $\gamma_2$, and $\beta_1$ and $\beta_2$. In addition to the bifurcation diagrams for each individual parameter, we also present joint bifurcation diagrams where the stereoselectivities are held constant for dimers and trimers (i.e., $\alpha_1 = \alpha_2$, $\gamma_1 = \gamma_2$, $\beta_1 = \beta_2$). These joint-parameter diagrams are useful for exploring the generality of oscillations, although it is worth noting that the stereoselectivities of peptide polymerization, epimerization, and hydrolysis are not necessarily independent of chain length [15].

In our bifurcation diagrams, we track the onset of oscillations through the concentration of the homochiral trimer DDD. In Figure 2a, for example, the upper line of points represents the maximum concentration of DDD at each value of $\alpha_1$—that is, the peak of the chemical oscillations—and the bottom represents the minimum concentration of DDD at each value of $\alpha_1$. The region of the graph where there is only one line (i.e., $[DDD]_{max}$=$[DDD]_{min}$), there are no oscillations. All bifurcation diagrams were created using an initial *ee* of 0.01.

Similar to the original APED model, oscillations in the trimer model depend on the preferential polymerization of heterochiral peptides. With the addition of trimers, though, the minimum values for heterochiral polymerization ($\alpha_1$ and $\alpha_2$) are significantly lower than that for the dimer model. The bifurcation diagram for $\alpha_1$ indicates that stable oscillations begin at around $\alpha_1$ = 5 for $\alpha_2$ = 20, which is more than 10 (dimensionless) units below the minimum value for $\alpha_1$ in the original APED model, which is just over 16. Similarly, Figure 2b depicts that the minimum value for $\alpha_2$ when $\alpha_1$ is held constant at 20 is just under 6, also well below the original APED's 16. Finally, in order to consider the case for which the rates of homo- and heterochiral polymerization are the same, the bifurcation diagram in Figure 2c indicates that the joint parameter bifurcates at 10, also significantly lower than in the original APED. Increasing the allowed range of values for heterochiral polymerization allows the model to apply to a wider range of real peptide-forming systems.

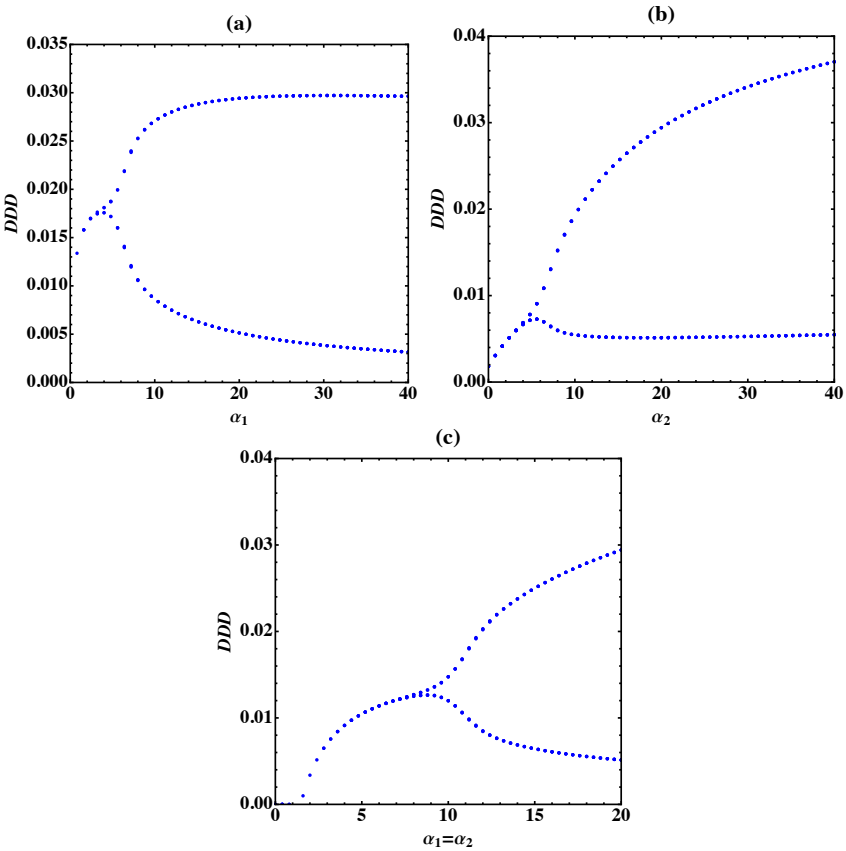


**Figure 2.** The bifurcation diagrams for $\alpha_1$ (**a**) and $\alpha_2$ (**b**) and the joint parameter where $\alpha_1 = \alpha_2$ (**c**) illustrate that heterodimers and heterotrimers must be formed preferentially for oscillations to occur. Other parameters are $a = p_1 = h_1 = e_1 = p_2 = h_2 = e_2 = 1$, $b = \beta_1 = \gamma_1 = \beta_2 = \gamma_2 = 0$, $\alpha_2 = 20$ (**a**), $\alpha_1 = 20$ (**b**), $c = 0.5$, $ee_{init} = 0.01$.

To check the impact of the stereoselectivity of epimerization, in Figure 3 we explore the bifurcation diagrams of $\gamma_1$, $\gamma_2$, and the joint parameter where they share the same value. Figure 3a illustrates that the region for stable oscillations closes around $\gamma_1 \approx 1.15$. The fact that the region extends past $\gamma_1 = 1$ indicates that stable oscillations occur even in the case of unity, which is the absence of any stereoselectivity of dimer epimerization. Similarly, in Figure 3b,c, which display the bifurcation diagrams for $\gamma_2$ and the joint parameter between $\gamma_1$ and $\gamma_2$, the regions of stable oscillations close at around $\gamma_2 \approx 1.5$ and $\gamma_1 = \gamma_2 \approx 1.15$, respectively. These diagrams suggest that epimerization need not be stereoselective for dimers nor trimers to produce oscillations.

The bifurcation diagrams in Figure 4 indicate that the allowed range of values for $\beta_1$, $\beta_2$, and the joint parameter where $\beta_1 = \beta_2$ close at 0.27, 0.95, and 0.23, respectively. These results suggest that the allowed range of values are more restricted for the stereoselectivities of hydrolysis. Despite this restrictiveness, Figure 4d displays another version of the joint bifurcation diagram for $\beta_1$ and $\beta_2$ but with the parameter values $h_1 = h_2 = 0.2$, $e_1 = e_2 = 0.1$. We note that a peptide system for which the rate of polymerization is faster than hydrolysis and hydrolysis is faster than epimerization is chemically realistic [15]. With this in mind, Figure 4d demonstrates that oscillations also occur in the absence of stereoselective hydrolysis for dimers and trimers.

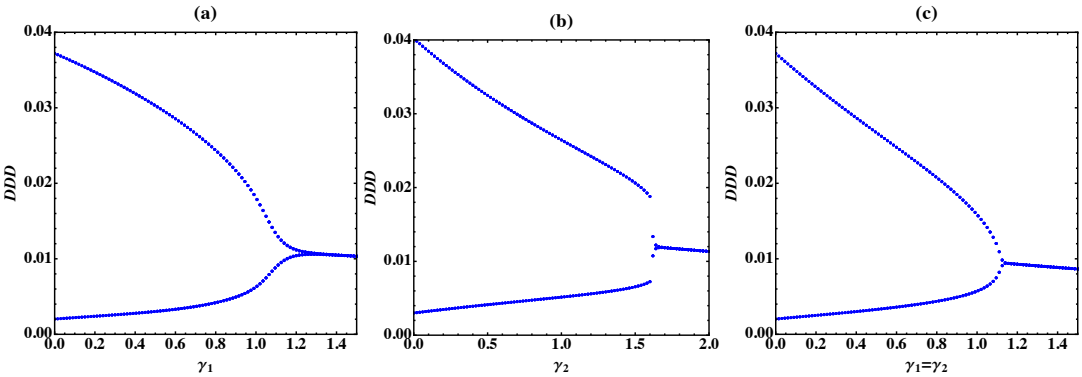


**Figure 3.** The bifurcation diagrams for $\gamma_1$ (**a**), $\gamma_2$ (**b**), and the joint parameter where $\gamma_1$=$\gamma_2$. Panel (**c**) illustrates the flexibility of the range of values for the stereoselectivity of epimerization that give rise to oscillations. Under these parameter values the range of allowed values for stereoselectivity of epimerization extend past unity. Other parameters are $a = p_1 = h_1 = p_2 = h_2 = e_2 = 1$, $b = \beta_1 = \beta_2 = \gamma_1 = \gamma_2 = 0$, $\alpha_1 = \alpha_2 = 50, e_1 = 0.5$ (**a**) and (**c**); $e_1 = 1$ (**b**), c = 0.5, $ee_{init} = 0.01$.

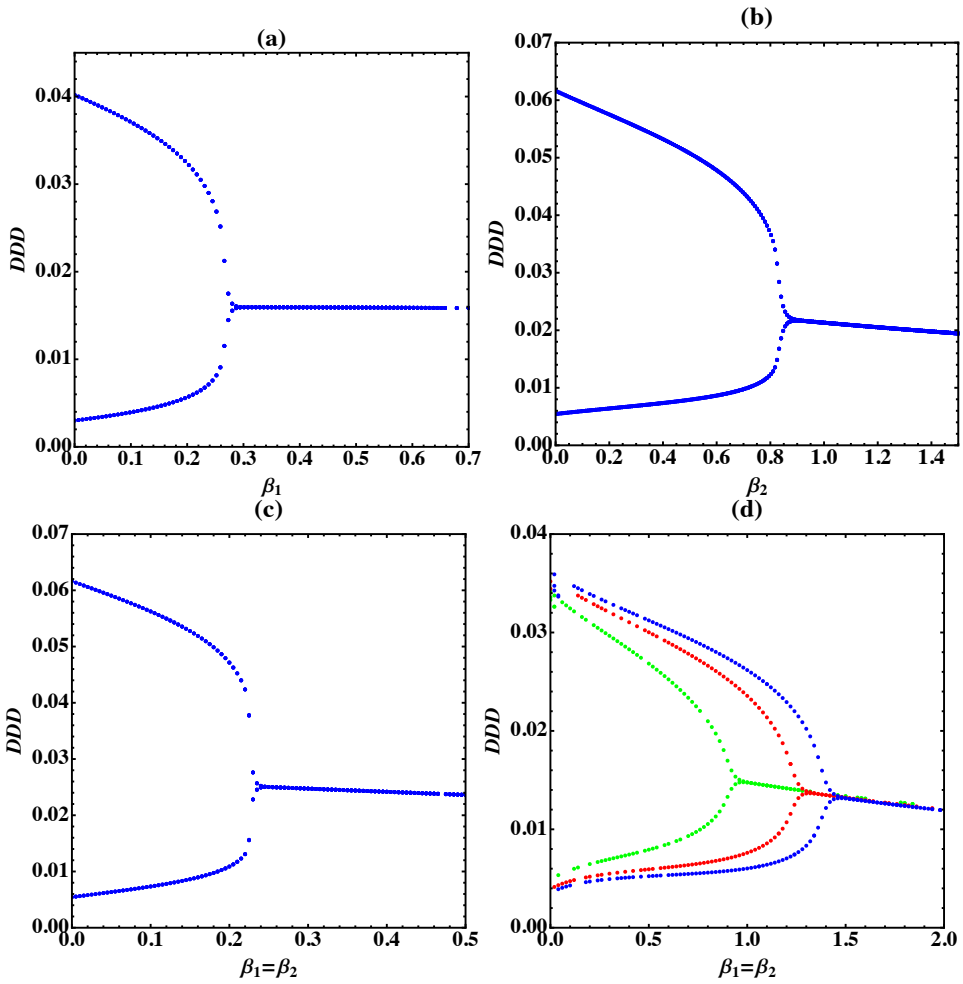


**Figure 4.** The bifurcation diagrams of $\beta_1$ (**a**), $\beta_2$ (**b**), and the joint parameter where $\beta_1$=$\beta_2$ (**c**) depicts the range of parameter values for the stereoselectivity of hydrolysis that result in oscillations. Under this set of parameter values, the range of allowed values is not as flexible for hydrolysis as for epimerization. Other parameters are $a = p_1 = h_1 = e_1 = p_2 = e_2 = 1$, $b = \gamma_1 = \gamma_2 = \beta_2 = 0$, $\alpha_1 = \alpha_2 = 50$, $h_2 = 1$ (**a**), $h_2 = 0.5$ (**b**), and (**c**), $c = 0.5$, $ee_{init} = 0.01$. Panel (**d**) is the joint bifurcation diagram of $\beta_1$ and $\beta_2$ with the parameters $h_1 = h_2 = 0.2, e_1 = e_2 = 0.1$. The three values are $\alpha_1 = \alpha_2 = 50$ (green), $\alpha_1 = \alpha_2 = 100$ (red), $\alpha_1 = \alpha_2 = 150$ (blue).

To conclude our bifurcation analysis for the trimer model, we explore the relationship between the stereoselectivities of hydrolysis and epimerization using an analogous parameter set to Figure 4d in order to find stable oscillations in the absence of any stereoselective epimerization and hydrolysis. Figure 5 shows the joint bifurcation diagrams of $\beta_1$ and $\gamma_1$ as well as $\beta_2$ and $\gamma_2$, that is, the case where the stereoselectivities of hydrolysis and epimerization are the same for dimers and trimers, respectively. Although these two stereoselectivities are not directly related chemically, the bifurcation diagrams illustrate that oscillations still occur if both heterochiral hydrolysis and epimerization are preferred for di- or tripeptides. Finally, in order to demonstrate oscillations in the absence of stereoselectivity for all hydrolysis and epimerization terms, Figure 5c revisits the joint bifurcation diagram for $\gamma_2$ and $\beta_2$, but with a parameter set for which $\gamma_1 = \beta_1 = 1$. For the other parameters, we choose $h_1 = h_2 = 0.1$ and $e_1 = e_2 = 0.02$ and we consider three values for $\alpha_1$ and $\alpha_2$. This specific example demonstrates that homochiral epimerization and depolymerization are not necessary conditions for sustained oscillations.

### 3.2. Tetramer and Pentamer Models

The bifurcation analysis in Section 3.1 shows that oscillations occur in the trimer APED model for a wide range of parameters. Here, we expand the model further to include homo- and heterochiral tetramers and pentamers in order to investigate the onset of oscillations in the presence of higher oligomers. The reactions we add include homochiral polymerization (rates $p_3$, $p_4$), heterochiral polymerization (rates $\alpha_3 p_3, \alpha_4 p_4$), homochiral hydrolysis (rates $h_3$, $h_4$), heterochiral hydrolysis (rates $\beta_3 h_3$, $\beta_4 h_4$), homochiral epimerization (rates $e_3$, $e_4$), and heterochiral epimerization (rates $\gamma_3 e_3$, $\gamma_4 e_4$). Instead of analyzing each individual parameter (as in Section 3.1), we focus our discussion on the joint parameters for polymerization, epimerization, and hydrolysis.

We find that the tetramer and pentamer models share many of the same characteristics as the minimal and trimer models. The bifurcation diagram in Figure 6a indicates that preferential formation of heterochiral oligomers is still necessary for oscillations, although the range of allowed values for the joint parameter for heterochiral polymerization closes at 7.75 for the tetramer model ($\alpha_1 = \alpha_2 = \alpha_3$) and 7.25 for the pentamer model ($\alpha_1 = \alpha_2 = \alpha_3 = \alpha_4$), each of which is less than the minimum values for the trimer model ($\alpha_1 = \alpha_2 = 10$) and minimal model ($\alpha_1 = 16$). This trend suggests that the requirement for strongly preferential heterochiral polymerization becomes less restrictive as oligomers of increasing length are incorporated into the system.

The bifurcation diagrams in Figure 6b,c indicate that, similar to the minimal and trimer models, the tetramer and pentamer models also favor homochiral epimerization and hydrolysis. Nevertheless, Figure 6b illustrates that the range of allowed values for the stereoselectivity of epimerization closes at 1.38 and 1.21 for the tetramer and pentamer models, respectively. The fact that both values extend past unity means that epimerization in both systems need not be stereoselective for oscillations to occur. Similarly, Figure 6c, which uses the analogous parameter set as in Figure 4d, demonstrates that oscillations occur in the absence of stereoselective hydrolysis for both the tetramer and pentamer models.

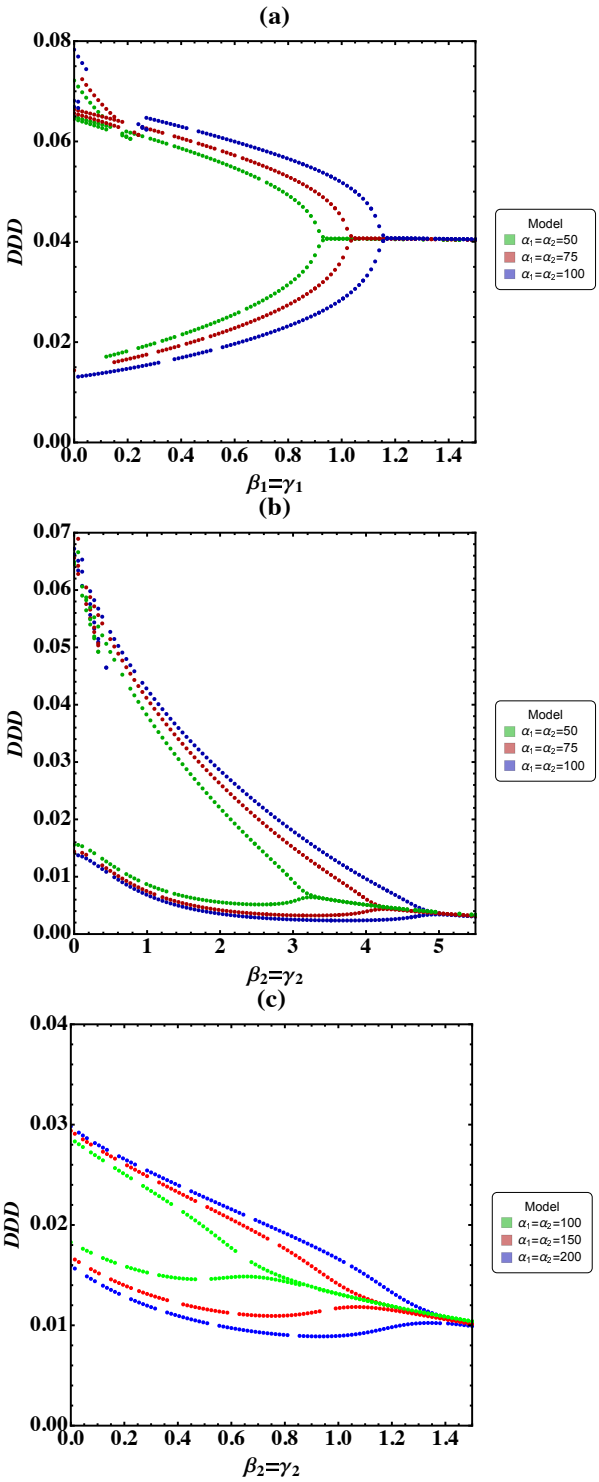


**Figure 5.** The joint bifurcation diagrams for $\gamma_1$ and $\beta_1$ (**a**) and $\gamma_2$ and $\beta_2$ (**b**) illustrate that sustained oscillations occur even when dimers or trimers favor homochiral epimerization and hydrolysis (i.e., $\gamma_1 = \beta_1 > 1,\ \gamma_2 = \beta_2 > 1$). Other parameters are $a = p_1 = p_2 = c = 1,\ h_1 = h_2 = 0.2, e_1 = e_2 = 0.1,\ \gamma_2 = \beta_2 = 0$ (**a**), $\gamma_1 = \beta_1 = 0$ (**b**), and $ee_{init} = 0.01$. Panel (**c**) is the joint bifurcation diagram for $\gamma_2$ and $\beta_2$ with a different set of parameters, including $\gamma_1 = \beta_1 = 1,\ h_1 = h_2 = 0.1\ e_1 = e_2 = 0.02$. This diagram shows that oscillations occur even in the absence of stereoselectivity for all hydrolysis and epimerization terms.

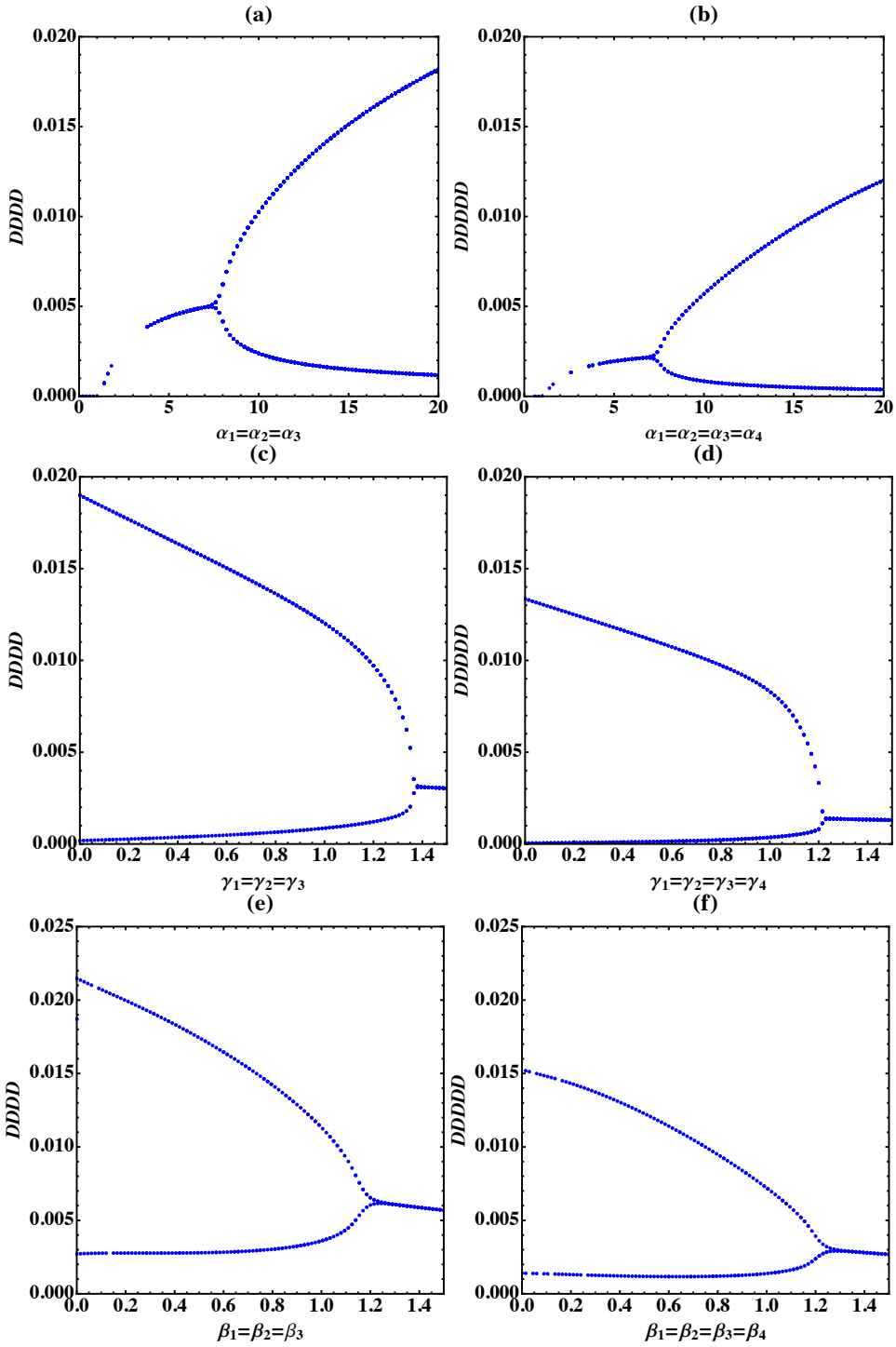


**Figure 6.** The joint bifurcation diagrams for the tetramer (left) and pentamer (right) activation—polymerization—epimerization—depolymerization (APED) models for polymerization (panels (**a**,**b**)), epimerization (panels (**c**,**d**)), and hydrolysis (panels (**e**,**f**)). Parameters in (**a**,**b**) are $a = p_{1,2,3,4} = h_{1,2,3,4} = e_{1,2,3,4} = 1$, $b = \beta_{1,2,3,4} = \gamma_{1,2,3,4} = 0$, $ee_{init} = 0.01$. Parameters in (**c**,**d**) are same as (**a**,**b**) except for $\alpha_{1,2,3,4} = 50$ and $e_{1,2,3,4} = 0.5$, and parameters in (**e**,**f**) are the same as (**c**,**d**) except for $e_{1,2,3,4} = 0.1$ and $h_{1,2,3,4} = 0.2$.

## 4. Minimum Initial Enantiomeric Excess

Here, we explore the minimum initial enantiomeric excess (*ee*) required for oscillations in the minimal and expanded APED models. For the APED model and its expansions studied in this report,

each unique oscillation-producing parameter set results in oscillations of a certain amplitude, and above a critical value, the amplitude of the oscillations is independent of the initial excess. If, on the other hand, the initial excess is below the critical value, then the system reaches a dead state where none of the concentrations oscillate. Analysis of the minimum initial *ee* is relevant when considering a chemical system's capacity to undergo spontaneous mirror symmetry breaking, because systems with smaller minimums will respond to more subtle chiral perturbations, such as statistical chiral fluctuations or external chiral influences.

Throughout our analysis, in order to standardize the conditions for each system, we set the rates and stereoselectivities of polymerization, epimerization, and hydrolysis equal across all models. We also hold the concentrations of each system to $c$ = 1. We first look at the cases for which $\alpha_1 = \alpha_2 = \alpha_3 = \alpha_4 =$ 25, 50, 75, 100, 125, and 150, and the graph of our results is presented in Figure 7a. We find that the minimum initial *ee* depends on chain length for all values of $\alpha_1 = \alpha_2 = \alpha_3 = \alpha_4$, and the critical value generally decreases as chain length increases. The exception to this trend occurs at $\alpha_1 = \alpha_2 = \alpha_3 = \alpha_4 = 125$ where the minimum value of the tetramer model falls to $20^{-10.8}$ compared to $20^{-9}$ in the pentamer model. Of the parameter sets studied, the minimum initial *ee* for the pentamer model is on average 2.5 orders of magnitude lower than that of the minimal model.

In Figure 7b, we check the impact of the stereoselectivity of epimerization on the minimum initial *ee* and find a similar trend to Figure 7a. Namely, the critical value generally decreases as chain length increases, especially for low values of $\gamma_1 = \gamma_2 = \gamma_3 = \gamma_4$ (i.e., when homochiral epimerization is more strongly favored). The exceptions to this trend occur at $\gamma_1 = \gamma_2 = \gamma_3 = \gamma_4 = 0.3$ where the minimum initial excess for the trimer model drops below that of the tetramer model, and at $\gamma_1 = \gamma_2 = \gamma_3 = \gamma_4 = 0.5$ where the critical values for both the trimer and tetramer models fall below that of the pentamer model.

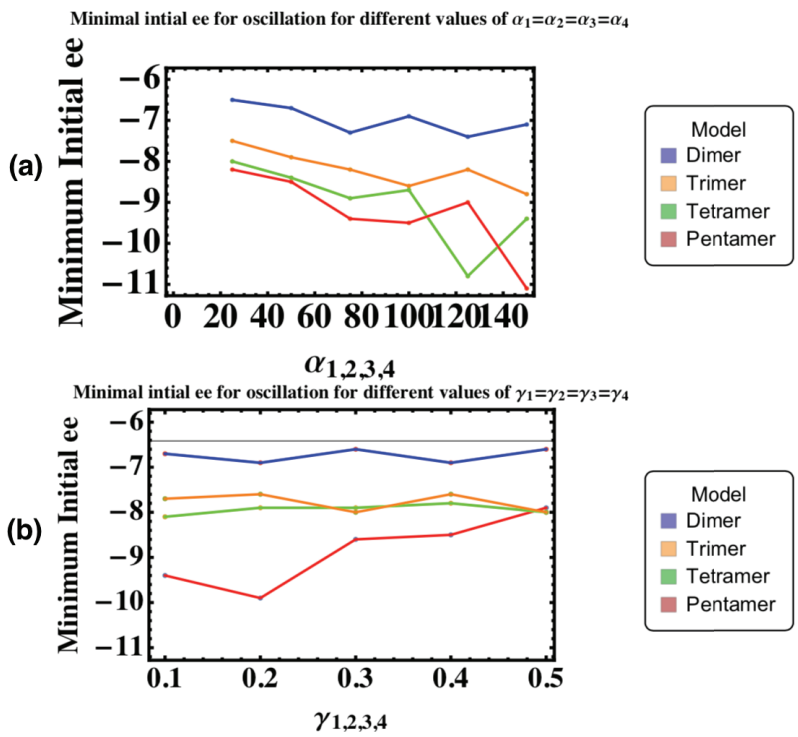


**Figure 7.** Plots of the minimum initial enantiomeric excesses (ee) required for oscillations and amplification in the minimal and expanded APED models for varying $\alpha_1 = \alpha_2 = \alpha_3 = \alpha_4$ (**a**) and varying $\gamma_1 = \gamma_2 = \gamma_3 = \gamma_4$ (**b**). Other parameters are $a = p_{1,2,3,4} = h_{1,2,3,4} = c = 1$, $e_{1,2,3,4} = 0.5$, $b = \beta_{1,2,3,4} = \gamma_{1,2,3,4} = 0$, and all other stereoselectivities (represented by greek letters) are zero. Parameters for (**b**) are same as (**a**) with $\alpha_{1,2,3,4} = 50$.

This preliminary analysis demonstrates that the initial *ee* required for oscillations and chiral amplification in the APED model depends both on the specific parameter set and the length of the largest oligomer allowed in the system.

Finally, to complete our study, we explore the amplitudes and periods of oscillations in the overall enantiomeric excess for the minimal and expanded APED models (Figure 8). For parameters we choose $\alpha_1 = \alpha_2 = \alpha_3 = \alpha_4 = 50$, $e_1 = e_2 = e_3 = e_4 = 0.5$, $c = 0.35$ and $ee_{init} = 10^{-6}$, and we see that the amplitude of the chiral oscillations increases as higher oligomers are introduced to the system. Specifically, oscillations in the dimer model range from $-0.62$ to 0.62, compared to $-0.98$ to 0.98 in the pentamer model. Furthermore, we also observe an inverse relationship between oligomer length and frequency, and the period of oscillations in the pentamer model is more than three times that of the dimer one.

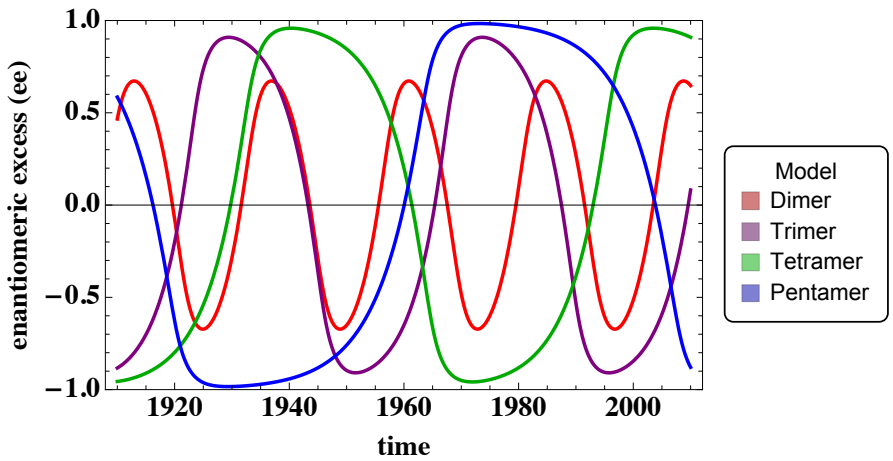


**Figure 8.** Oscillations in overall enantiomeric excess for the minimal and expanded APED models. Each simulation began with an initial *ee* of $10^{-6}$, and the amplitudes of the oscillations for each model are as follows; dimer: $-0.62$, 0.62; trimer: $-0.91$, 0.91; tetramer: $-0.96$, 0.96; pentamer: $-0.98$, 0.98. Other parameters are $a = p_{1,2,3,4} = h_{1,2,3,4} = 1$, $e_{1,2,3,4} = 0.5$, $b = \beta_{1,2,3,4} = \gamma_{1,2,3,4} = 0$, $\alpha_{1,2,3,4} = 50$, $c = 0.35$. Similarly to Figure 1, the units of time are dimensionless.

## 5. Conclusions

In this paper, we have expanded the minimal APED model to include trimers, tetramers, and pentamers and have studied the range of parameter sets leading to chiral oscillations. In particular, we have analyzed the bifurcation diagrams of several system parameters including the stereoselectivities of polymerization, epimerization, and hydrolysis. We have also begun an investigation of the minimum initial enantiomeric excess required to produce oscillations in the minimal and expanded models.

Principally, we find that oscillations in the expanded APED models have similar properties to those in the original one: namely, oscillations are favored for heterochiral polymerization and homochiral depolymerization and epimerization. Additionally, we show that stable oscillations occur for a wide range of parameters. In particular, $\beta_1$, $\beta_2$, $\beta_3$, and $\beta_4$ as well as $\gamma_1$, $\gamma_2$, $\gamma_3$, and $\gamma_4$ can also be chosen at unity, indicating that hydrolysis and epimerization need not be stereoselective for oscillations to occur. On the other hand, heteropolymers still need to be formed preferentially, although the allowed range of values for $\alpha_1$, $\alpha_2$, $\alpha_3$, and $\alpha_4$ extends closer to unity with the inclusion of higher oligomers.

In addition to analyzing the effects of the stereoselectivities of polymerization, epimerization and hydrolysis on oscillations, using the trimer model we also explore the onset of oscillations as the stereoselectivities of hydrolysis and epimerization both approach unity. Although preferential homochiral epimerization and hydrolysis are favorable for oscillations, we show that oscillations occur even when all hydrolysis and epimerization terms are chosen at unity. While these rates are not directly related, this observation is noteworthy in light of experimental evidence suggesting that

amino acid chains favor heterochiral epimerization and hydrolysis [15]. Moreover, we find that the range of allowed values for the stereoselectivities of epimerization and hydrolysis expands when those values vary with chain length. This is a significant observation when taking into consideration Danger et al.'s observation that homochiral chains are stabilized as chain length increases [15], meaning that in real systems of amino acids, even if $\gamma_1$ and $\beta_1$ must be greater than unity, $\gamma_{2,3,4}$ and $\beta_{2,3,4}$ are likely closer to unity, if not below.

Aside from the bifurcation analysis, another important property of any system involving SMSB—oscillatory or otherwise—is the minimum initial enantiomeric excess required to activate its propagation. We show that this critical value depends on the parameter set and the chain length of the longest polymer in the system. We also demonstrate that the critical value can be significantly lower when higher oligomers are incorporated into the system, although further investigation will be needed to determine the full effect of chain length.

Additionally, we show that chain length affects the amplitude and frequency of oscillations in the overall *ee*, and that the APED system produces more robust and longer lasting oscillations as higher oligomers are introduced. This discrepancy in amplitude is caused in large part by the fact that the hetero-oligomers in the dimer model are achiral, while those in the expanded models are not. This is because for the heterodimers LD and DL, the two enantiomers cancel each other out. In the expanded models, however, even though the two terminal monomers on the heterochiral chains still cancel each other out, the remaining ones contribute to the overall chirality in the system. As a result, each hetero-trimer contributes one molecule of chirality, the hetero-tetramers contribute two and the hetero-pentamers contribute three. Accordingly, the pentamer model experiences the largest amplitude oscillations, and it can temporarily, and periodically, achieve near homochirality from a small initial enantiomeric excess of $10^{-6}$. Such large amplitude chiral oscillations have been studied previously in a polymerization model closed to matter and energy flow, in which the length of the homochiral chain formed determines the amplitude of the chiral oscillations [13]. They have also been demonstrated in a theoretical model designed to model symmetry breaking in the Soai reaction [20]. The amplitude, period, and minimum initial *ee* for oscillations are all important features when considering a chemical system's ability to amplify small chiral perturbations—whether they be caused by the presence of chiral crystals such as sodium chlorate [21], circularly polarized light [22], or another external chiral influence—in a prebiotic environment.

**Author Contributions:** Conceptualization, E.P.-L. and W.B.; methodology, E.P.-L.; software, W.B. and E.P.-L.; validation, W.B., E.P.-L.; formal analysis, W.B.; investigation, W.B.; resources, E.P.-L.; writing—original draft preparation, W.B.; writing—review and editing, W.B. and E.P.-L.; supervision, E.P.-L.; project administration, E.P.-L.; funding acquisition, E.P.-L. All authors have read and agreed to the published version of the manuscript.

**Funding:** This research received no external funding.

**Acknowledgments:** The authors would like to acknowledge the support from the summer research program at Williams College.

**Conflicts of Interest:** The authors declare no conflict of interest.

## References

1. Frank, F.C. On spontaneous asymmetric synthesis. *Biochim. Biophys. Acta* **1953**, *11*, 459–463. [CrossRef]
2. Soai, K.; Shibata, T.; Morioka, H.; Choji, K. Asymmetric autocatalysis and amplification of enantiomeric of a chiral molecule. *Nature* **1995**, *378*, 767–768. [CrossRef]
3. Ribo, J.M.; Hochberg, D. Stability of racemic and chiral steady states in open and closed chemical systems. *Phys. Lett. A* **2008**, *373*, 111–122. [CrossRef]
4. Blackmond, D.G. Asymmetric amplification and its implications for the origin of homochirality. *Proc. Natl. Acad. Sci. USA* **2004**, *101*, 5732–5736. [CrossRef]
5. Islas, J.R.; Lavabre, D.; Grevy, J.M.; Lamoneda, R.H.; Cabrera, H.R.; Micheau, J.C.; Buhse, T. Mirror-symmetry breaking in the Soai reaction: A kinetic understanding. *Proc. Natl. Acad. Sci. USA* **2005**, *102*, 13743–13748. [CrossRef]

6. Sandars, P.G.H. A toy model for the generation of homochirality during polymerization. *Orig. Life Evol. Biosph.* **2003**, *33*, 575–587. [CrossRef]
7. Brandenburg, A.; Anderson, A.C.; Höfner, S.; Nilsson, M. Homochiral growth through enantiomeric cross inhibition. *Orig. Life. Evol. Biosph.* **2005**, *35*, 225–241. [CrossRef]
8. Brandenburg, A.; Anderson, A.C.; Höfner, S.; Nilsson, M. Dissociation in a polymerization model of homochirality. *Orig. Life. Evol. Biosph.* **2005**, *35*, 507–521. [CrossRef]
9. Wu, M.; Walker, S.I.; Higgs, P.G. Autocatalytic replication and homochirality in biopolymers: Is homochirality a requirement of life or a result of it? *Astro* **2012**, *12*, 818–829. [CrossRef]
10. Plasson, R.; Bersisni, H.; Commeyras, A. Recycling Frank: Spontaneous emergence of homochirality in noncatalytic systems. *Proc. Natl. Acad. Sci. USA* **2004**, *48*, 16733–16738. [CrossRef]
11. Brandenburg, A.; Lehto, H.J.; Lehto, K.M. Homochirality in an early peptide world. *Astro* **2007**, *7*, 725–732. [CrossRef] [PubMed]
12. Stich, M.; Blanco, C.; Hochberg, D. Chiral and chemical oscillations in a simple dimerization model. *Phys. Chem. Chem. Phys.* **2013**, *15*, 255–261. [CrossRef] [PubMed]
13. Blanco, C.; Hochberg, D. Chiral polymerization: symmetry breaking and entropy production in closed systems. *Phys. Chem. Chem. Phys.* **2011**, *13*, 839–849. [CrossRef] [PubMed]
14. Sajewicz, M.; Gontarska, M.; Kronenbach, D.; Leda, M.; Kowalska, T.; Epstein, I.R. Condensation oscillations in the peptidization of phenylglycine. *J. Syst. Chem.* **2010**, *1*, 651–662. [CrossRef]
15. Danger, G.; Plasson, R.; Pascal, R. An experimental investigation of the evolution of chirality in a potential dynamic peptide system: N-terminal epimerization and degradation into diketopoperazine. *Phys. Chem. Chem. Phys.* **2010**, *6*, 255–261. [CrossRef]
16. Lundberg, R.D.; Doty, P. Configurational and stereochemical effects in the amine-initiated polymerization of n-carboxy-anhydrides. *J. Am. Chem. Soc.* **1956**, *78*, 4810–4812.
17. Bartlett, P.D.; Jones, R.H. A kinetic study of leuchs anhydrides in aqueous solution. *J. Am. Chem. Soc.* **1957**, *79*, 2153–2159. [CrossRef]
18. Mauksch, M.; Tsogoeva, S.B. Life's Single Chirality: Origin of Symmetry Breaking in Biomolecules. In *Biomimetic Organic Synthesis*; Poupon, E., Nay, B., Eds.; WILEY-VCH: Weinheim, Germany, 2011; Volume 2, pp. 823–846.
19. Joyce, G.F.; Visser, G.M.; van Boeckel, C.A.A.; van Boom, J.H.; Orgel, L.E.; van Westrenen, J. Chiral selection in poly(C)-directed synthesis of oligo(G). *Nature* **1984**, *310*, 602–604. [CrossRef]
20. Micskei, K.; Rabai, G.; Gal, E.; Caglioti, L.; Palyi, G. Oscillatory symmetry breaking in the Soai reaction. *J. Phys. Chem. B* **2008**, *14*, 9196–9200. [CrossRef]
21. Sato, I.; Kadowaki, K.; Ohgo, Y.; Soai, K. Highly enantioselective autocatalysis induced by chiral ionic crystals of sodium chlorate and sodium bromate. *J. Mol. Catal. A Chem.* **2004**, *216*, 209–214. [CrossRef]
22. Bonner, W.A.; Bean, B.D. Asymmetric photolysis with elliptically polarized light. *Orig. Life Evol. Biosph.* **2000**, *30*, 513–517. [CrossRef] [PubMed]


© 2020 by the authors. Licensee MDPI, Basel, Switzerland. This article is an open access article distributed under the terms and conditions of the Creative Commons Attribution (CC BY) license (http://creativecommons.org/licenses/by/4.0/).